King Saud University

Journal of Saudi Chemical Society

www.ksu.edu.sa
www.sciencedirect.com

ORIGINAL ARTICLE

Kinetics and mechanism of the reduction of colloidal MnO$_2$ by glycyl-leucine in the absence and presence of surfactants

Mohd. Akram [a], Mohammad Altaf [a], Kabir-ud-Din [a],*, Shaeel Ahmed Al-Thabaiti [b]

[a] Department of Chemistry, Aligarh Muslim University, Aligarh 202002, UP, India
[b] Faculty of Science, King Abdul Aziz University, P.O. Box 80203, Jeddah 21413, Saudi Arabia

Abstract The kinetics of the reduction of water-soluble colloidal manganese dioxide by glycyl-leucine (Gly-Leu) has been investigated in the presence of perchloric acid both in aqueous as well as micellar media at 35 °C. The study was carried out as functions of [MnO$_2$], [Gly-Leu] and [HClO$_4$]. The first-order-rate is observed with respect to [MnO$_2$], whereas fractional-order-rates are determined in both [Gly-Leu] and [HClO$_4$]. Addition of sodium pyrophosphate and sodium fluoride enhanced the rate of the reaction. Further, the use of surfactant micelles is highlighted as, in favourable cases, the micelles help the redox reactions by bringing the reactants into a close proximity due to hydrogen bonding. While the ionic surfactants SDS and CTAB have not shown any effect on the reaction rate, the nonionic surfactant TX-100 has catalytic effect which is explained in terms of the mathematical model proposed by Tuncay et al. (1999). The Arrhenius and Eyring equations are valid for the reaction over the range of temperatures used and different activation parameters (E_a, $\Delta H^{\#}$, $\Delta S^{\#}$ and $\Delta G^{\#}$) have been evaluated. Kinetic studies show that the redox reaction between MnO$_2$ and Gly-Leu proceeds through a mechanism combining one- and two-electron pathways: Mn(IV) $\rightarrow$ Mn(III) $\rightarrow$ Mn(II) and Mn(IV) $\rightarrow$ Mn(II). On the basis of the observed results, a possible mechanism has been proposed and discussed.

* Corresponding author.
E-mail address: kabir7@rediffmail.com (Kabir-ud-Din).

Production and hosting by Elsevier

1. Introduction

Peptides and proteins are the most characteristic chemical compounds found in living cells. They are composed of amino acids. The oxidation of amino acids as well as oxidation of peptides and proteins has been studied by many workers (Stadtman, 1993; Davies, 1987; Davies et al., 1987; Giulivi and Davies, 1993, 2001). Protein oxidation can occur at both the protein backbone and on the amino acid side chains, with the ratio of attack dependent on the nature of the oxidants (Deans et al., 1997; Davies, 2005). Therefore, the nature of the radicals formed on peptides and proteins depends on the

reactivity of the oxidant and its electrophilicity and nucleophilicity. It is well established that protein oxidation is a significant consequence of oxidative stress, in addition to free-radical-mediated damage of DNA and lipids. Oxidative modification to proteins (by reactive oxygen and nitrogen species) is often accompanied by unfolding of the protein and loss of enzymatic function. If such protein oxidation products are not removed rapidly, they tend to accumulate in cells and may contribute to the formation of large, cross-linked aggregates, which can threaten cell function and viability. Cells have, therefore, developed efficient enzymatic systems for the removal of oxidatively damaged proteins. Such rapid removal of oxidized proteins by degradation constitutes an important antioxidant defense strategy.

Manganese dioxide is a kind of attractive inorganic material, and material scientists have made great efforts on the synthesis of MnO_2 (Wang and Li, 2002, 2003; Wang et al., 2006; Xiong et al., 2003). Although heterogeneous reaction conditions are suitable for synthetic chemistry, the insolubility of manganese dioxide in water has limited its analytical application. However, the formation of soluble manganese(IV) complexes with various inorganic and organic species has been explored (Richens et al., 1979; Pastor and Pastor, 2000). Under certain conditions, permanganate can be reduced to give a reasonably stable, soluble form of manganese dioxide (Brown et al., 2007; Perez-Benito et al., 1989, 1996; Perez-Benito and Arias, 1992; Jáky et al., 1984; Jáky and Zrinyi, 1993; Barnett et al., 2001). The exact nature of this species has been the subject of debate, due in part to its dependence on the method of preparation, chemical environment and storage conditions. Perez-Benito et al. treated permanganate with a variety of reducing agents in near-neutral aqueous conditions to produce transparent dark-brown solutions containing colloidal manganese dioxide, which did not precipitate during several months of investigation (Perez-Benito et al., 1989, 1996; Perez-Benito and Arias, 1992). Coagulation experiments revealed a negative electrostatic charge, indicating that the stability of the particles was due to the adsorption of anions on their surface (Perez-Benito et al., 1989). Ninety percent of the particles in an MnO_2 sol prepared in this manner were found to have a diameter between 89 nm and 193 nm (Perez-Benito et al., 1996). Consequently, colloidal manganese dioxide with organic substrates has been studied in some depth focusing on the determination of kinetic parameters (Perez-Benito et al., 1989, 1996; Kabir-ud-Din et al., 2004, 2005; Khan et al., 2004). Some reports are also available on the oxidation of amino acids by colloidal MnO_2 in the absence (Ilyas et al., 2007; Andrabi and Khan, 2007; Kabir-ud-Din et al., 2008; Herszage et al., 2003) and presence (Akram et al., 2007; Altaf et al., 2009) of surfactants.

Surfactants are amphipathic molecules with both hydrophobic and hydrophilic properties. Micelles and vesicles are formed by self-aggregation of amphiphilic molecules in aqueous medium above the critical micelle concentration (cmc). The driving force of the formation of amphiphilic assemblies in water is the hydrophobic effect that means the increase of entropy owing to the dehydration of the hydrocarbon chain (Blokzijl and Engberts, 1993). The headgroup of the surfactants can be anionic, cationic, zwitterionic, or nonionic. The acceleration of a chemical reaction in the presence of micelles is called "micellar catalysis". Micellar catalysis can be due to environmental changes decreasing the free energy difference between the initial

and the transition states and also due to an increase in the frequency of molecular collisions as a consequence of the close association of the reactants at the micellar interface. So the activation energy plays a role in micellar catalysis.

We hereby investigate the reduction of colloidal manganese dioxide by glycyl-leucine (Gly-Leu) in the absence and presence of surfactants. Since MnO_2 is one and two electron oxidant and is also able to abstract H-atom from the peptide, this is good candidate to generate *in vitro* several of the organic radicals involved in the biological processes.

2. Experimental

2.1. Material

Glycyl-leucine, Gly-Leu (Acros, USA), potassium permanganate (98.5%, E. Merck, India), sodium thiosulfate (99%, s.d. fine, India), sodium fluoride (97%, BDH, India), tetrasodium pyrophosphate (99%, E. Merck, India), cetyltrimethylammonium bromide, CTAB (99%, BDH, UK), sodium dodecyl sulfate, SDS (99%, Sigma, USA) and poly(oxyethylene)-*t*-octylphenyl ether, TX-100 (99%, Fluka, Switzerland) were used as received. The solutions were prepared in deionized and double distilled water. Perchloric acid (70%, E. Merck, India) was used to maintain the $[H^+]$ constant.

2.2. Preparation of colloidal manganese dioxide

To prepare the stock solution of colloidal MnO_2, standardized $KMnO_4$ ($= 10.0$ cm^3, 0.1 mol dm^{-3}) and sodium thiosulfate ($= 20.0$ cm^3, 1.88×10^{-2} mol dm^{-3}) were used (Perez-Benito and Arias, 1992; Perez-Benito et al., 1996). The resulting solution was dark brown and perfectly transparent and remained stable for several weeks. In order to confirm the formation of water-soluble colloidal MnO_2, the fulfillment of the Beer–Lambert law by the resulting solution was checked. A calibration graph was constructed between absorbance and concentration of colloidal MnO_2 and the law was well obeyed for the concentration range used in the present investigations.
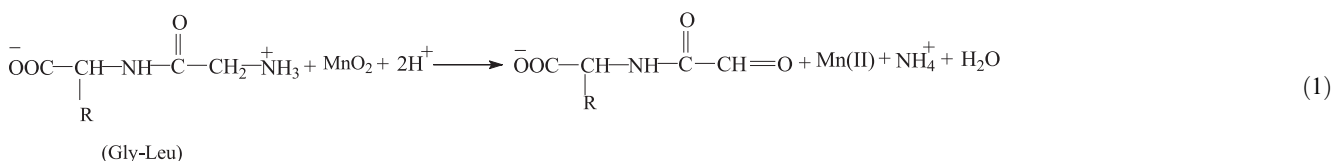
2.3. Kinetic studies

All kinetic measurements were performed under pseudo-first order conditions with Gly-Leu in at least a 10-fold molar excess over colloidal manganese dioxide (i.e., pseudo-order condition). The reaction mixture was placed in a water bath thermostated at the desired temperature (± 0.1 °C). After allowing sufficient time to attain the bath temperature, the reaction was initiated by adding the requisite amount of colloidal MnO_2 (placed separately in the same water bath). The course of the reaction was followed by monitoring the decrease in absorbance of colloidal MnO_2 in a 1 cm quartz cell of a Spectronic 20D(+) UV–vis spectrophotometer. The values of pseudo-first order rate constants were estimated from the slope of log(absorbance) vs. time plots. The effect of dissolved oxygen on the reaction rate was checked by preparing the reaction mixture and following the reaction in N_2-atmosphere. No significance difference between the results obtained under N_2 and in the presence of air was observed.

3. Results and discussion

3.1. Stoichiometry and products identification

Several reaction mixtures with [MnO$_2$] $\gg$ [Gly-Leu] were prepared and kept for 8 h at room temperature to determine the stoichiometry of the reaction. The unconsumed MnO$_2$ was then analyzed spectrophotometrically. The results indicated that one mole of MnO$_2$ was consumed by one mole of Gly-Leu according to following Eq. (1):

$$\overset{-}{OOC}-\underset{\underset{R}{|}}{CH}-NH-\overset{\overset{O}{\|}}{C}-CH_2-\overset{+}{NH_3} + MnO_2 + 2H^+ \longrightarrow \overset{-}{OOC}-\underset{\underset{R}{|}}{CH}-NH-\overset{\overset{O}{\|}}{C}-CH=O + Mn(II) + NH_4^+ + H_2O \tag{1}$$

(Gly-Leu)

where R = –CH$_2$CH(CH$_3$)$_2$.

Aldehyde and ammonia were identified as the end products of the reaction, which were confirmed by the following methods.

3.2. Identification of aldehyde

At the end of the reaction, a drop of reaction mixture was taken on a spot plate and a few drops of chlorite solution was added followed by a drop of 0.1 N hydrochloric acid, an yellow color appeared within 1 min; indicating that aldehyde was formed as end product of the reaction.

3.3. Identification of NH$_3$

Under the kinetic measurements, N$_2$ gas was bubbled through the reaction mixture. The evolved NH$_3$ was thus swept out and absorbed in Nessler's reagent. The appearance of yellow precipitate in Nessler's reagent showed the formation of NH$_3$ as the product.

3.4. Test for free radicals

To see the formation of free radicals as an intermediate in the redox reaction between the reactants, the reaction mixture was mixed with an acrylonitrile monomer and kept for 24 h in an inert atmosphere. On dilution with methanol, a white precipitate was formed, showing the presence of free radicals.

4. Reaction in absence of surfactants

Results of the reduction of colloidal MnO$_2$ by Gly-Leu are summarized as follows:

1. To get the order of the reaction with respect to Gly-Leu concentration, kinetic runs were carried out with varied concentration of Gly-Leu at 35 °C keeping the concentrations of

Table 1 Dependence of rate constant on the factors influencing the reduction of colloidal MnO$_2$ by Gly-Leu.

10^3 [Gly-Leu] (mol dm^{-3})	10^5 [MnO$_2$] (mol dm^{-3})	10^4 [HClO$_4$] (mol dm^{-3})	Temperature (°C)	10^4 k_{obs} (s^{-1})
1.0	4.0	2.0	35	1.1
2.0				2.0
4.0				2.5
6.0				2.8
8.0				3.3
10.0				3.5
4.0	2.0	2.0	35	4.0
	4.0			2.5
	6.0			2.3
	8.0			2.1
	10.0			2.1
4.0	4.0	1.0	35	2.2
		2.0		2.5
		4.0		2.7
		6.0		2.9
		8.0		3.2
		10.0		3.6
4.0	4.0	2.0	30	1.8
			35	2.5
			40	3.6
			45	4.8
			50	7.7

Activation parameters

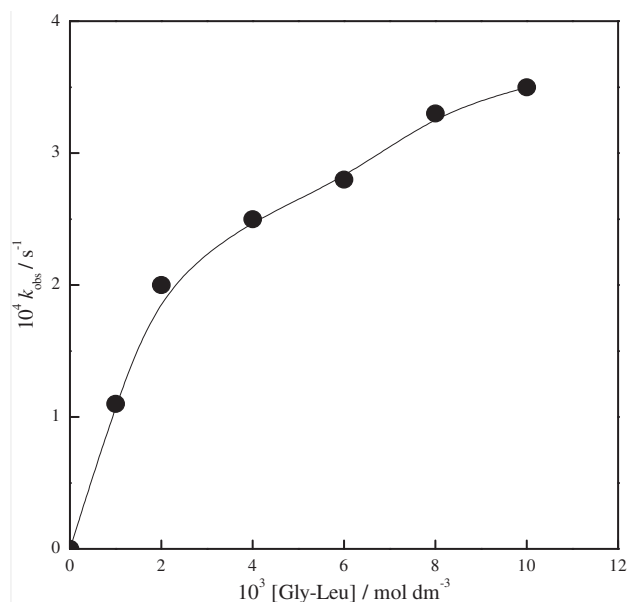|	
E_a (kJ mol^{-1})	60
$\Delta H^{\#}$ (kJ mol^{-1})	57
$\Delta S^{\#}$ (J K^{-1} mol^{-1})	−175
$\Delta G^{\#}$ (kJ mol^{-1})	111

Figure 1 Effect of [Gly-Leu] on the pseudo-first-order rate constant for the reduction of colloidal MnO$_2$ by Gly-Leu. *Reaction conditions*: [MnO$_2$] = 4.0 × 10^{-5} mol dm^{-3}, [HClO$_4$] = 2.0 × 10^{-4} mol dm^{-3}, temperature = 35 °C.

other reagents constant ($[MnO_2] = 4.0 \times 10^{-5}$ mol dm^{-3}, $[HClO_4] = 2.0 \times 10^{-4}$ mol dm^{-3}). The k_{obs} value (Table 1) increases with increase in [Gly-Leu]. The plot of k_{obs} vs. [Gly-Leu] is nonlinear passing through the origin (Fig. 1). The linear plot between log k_{obs} vs. log [Gly-Leu] yields a slope equal to 0.47 ($r = 0.976$), showing fractional-order in [Gly-Leu].

2. As indicated from the data in Table 1, the rate constant decreases with an increase in the concentration of colloidal manganese dioxide at 35 °C (at constant concentrations of Gly-Leu, and HClO$_4$). The decrease in rate constant may be due to the flocculation of the colloidal MnO$_2$ particles. As the MnO$_2$ concentration increases, the rate constants become independent on the initial MnO$_2$ concentration (Khan et al., 2004), which is due to the fast adsorption of Gly-Leu on the surface of colloidal MnO$_2$. This is not surprising: judging from the fact that the presence of negative charge on the surface of colloidal MnO$_2$ would provide the site most susceptible to be attacked by the positively charged Gly-Leu.

3. To see the role of [HClO$_4$] on the reaction rate, a series of kinetic runs were carried out with fixed MnO$_2$ and Gly-Leu concentrations at 35 °C (Table 1). The plot of rate constant vs. [HClO$_4$] shows a straight line with a positive intercept on the y-axis, indicating acid-independent and acid-dependent reaction paths being involved in the reduction of colloidal MnO$_2$ by Gly-Leu (Fig. 2). Double logarithm plot of rate constant and [HClO$_4$] was also linear with slope 0.19 ($r = 0.969$), which indicates fractional-order dependence on [HClO$_4$].

In view of the above points, the empirical rate law is written as:

$$-\frac{d[MnO_2]}{dt} = \{k_I + k_{II}[H^+]^{0.19}\}\,[MnO_2][Gly\text{-}Leu]^{0.47} \qquad (2)$$

4. All the above experiments were performed at a temperature of 35 °C. The dependence of k_{obs} with temperature was in agreement with the Arrhenius equation ($k = Ae^{-E_a/Rt}$, where A

is the preexponential factor, R is the gas constant, T is the absolute temperature, and E_a is the overall activation energy). The overall activation energy value obtained for Gly-Leu was 60.0 kJ mol^{-1} at constant [MnO$_2$], [Gly-Leu], and [HClO$_4$]. The overall activation energy for the rate constant (k_{obs}) will be a combination of the activation energies for elementary reactions. To determine whether the reaction mechanism is associative or dissociative, the entropy of activation is needed (Atwood, 1990), which was calculated from an Eyring plot [ln(k_{obs}/T) vs. 1/T] based on:

$$\ln(k_{obs}/T) = -(\Delta H^{\#}/RT) + \ln(k_B/h) + (\Delta S^{\#}/R) \qquad (3)$$

where $\Delta H^{\#}$ is the enthalpy of activation, $\Delta S^{\#}$ is the entropy of activation, k_B is the Boltzmann constant (1.381×10^{-23} J K^{-1}), and h is the Planck's constant (6.626×10^{-34} J s). The slope ($\Delta H^{\#}/R$) provides the enthalpy of activation, and the intercept $\{\ln(k_B/h) + (\Delta S^{\#}/R)\}$ yields the entropy of activation. Large negative value of $\Delta S^{\#}$ indicates an associative reaction whereas a large positive $\Delta S^{\#}$ value shows a dissociative reaction (Atwood, 1990). All kinetic activation parameters are given in Table 1, which show that MnO$_2$ has large negative $\Delta S^{\#}$ for MnO$_2$ reduction and that the reaction is associative and proceeds via inner-sphere redox reaction.

5. Pyrophosphate and fluoride ions are efficient trapping agents for Mn(III) (Davies, 1972; Littler, 1962; Girgis et al., 1985). Therefore, to confirm the presence of Mn(III) as an intermediate during the reduction of colloidal MnO$_2$ by Gly-Leu, a series of kinetic runs were made by adding different amounts of Na$_4$P$_2$O$_7$ and NaF at constant [Gly-Leu], [MnO$_2$], [HClO$_4$] and temperature (= 35 °C). As the concentration of trapping agents increase, the rate constants increase to a limit value and then decrease. The decreasing rate constant may be due to complex formation between manganese(III) and trapping agents. The results are shown
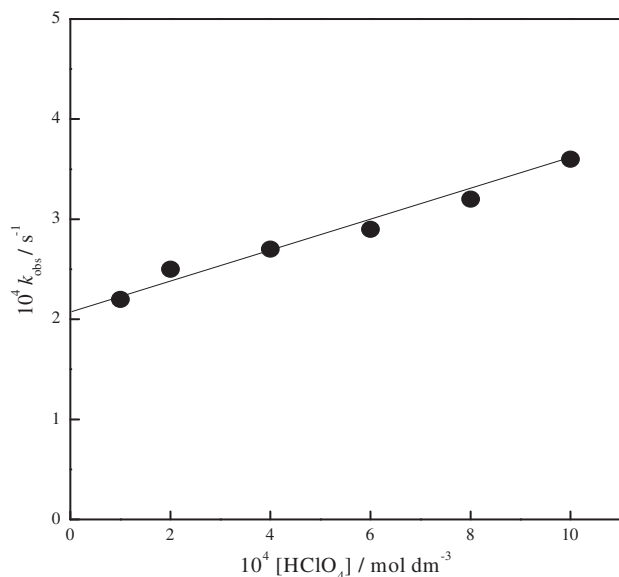

Figure 2 Effect of [HClO$_4$] on the pseudo-first-order rate constant for the reduction of colloidal MnO$_2$ by Gly-Leu. *Reaction conditions*: $[MnO_2] = 4.0 \times 10^{-5}$ mol dm^{-3}, [Gly-Leu] $= 4.0 \times 10^{-3}$ mol dm^{-3}, temperature $= 35$ °C.
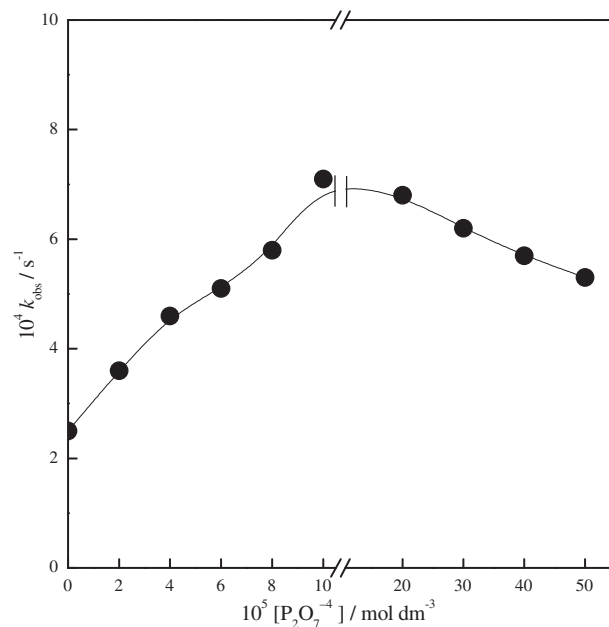

Figure 3 Effect of [P$_2$O$_7^{-4}$] on the pseudo-first-order rate constant for the reduction of colloidal MnO$_2$ by Gly-Leu. *Reaction conditions*: $[MnO_2] = 4.0 \times 10^{-5}$ mol dm^{-3}, [Gyl-Leu] $= 4.0 \times 10^{-3}$ mol dm^{-3}, [HClO$_4$] $= 2.0 \times 10^{-4}$ mol dm^{-3}, temperature $= 35$ °C.

Figure 4 Effect of [F$^-$] on the pseudo-first-order rate constant for the reduction of colloidal MnO$_2$ by Gly-Leu. *Reaction conditions*: [MnO$_2$] = 4.0 × 10^{-5} mol dm^{-3}, [Gly-Leu] = 4.0 × 10^{-3} mol dm^{-3}, [HClO$_4$] = 2.0 × 10^{-4} mol dm^{-3}, temperature = 35 °C.
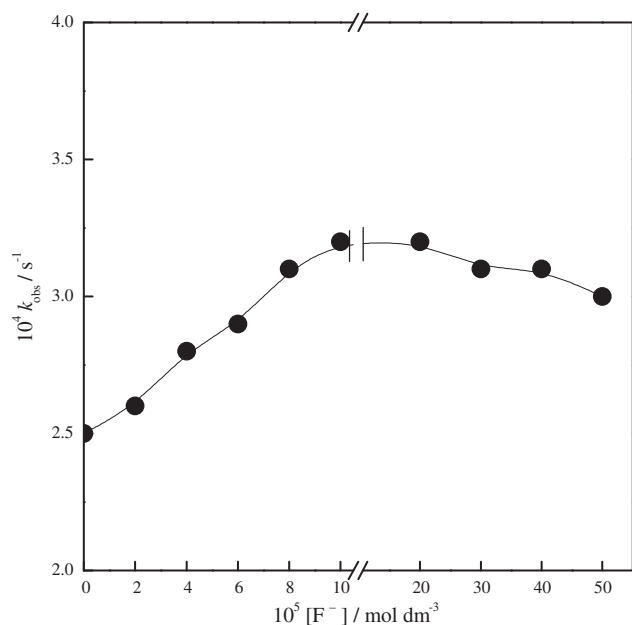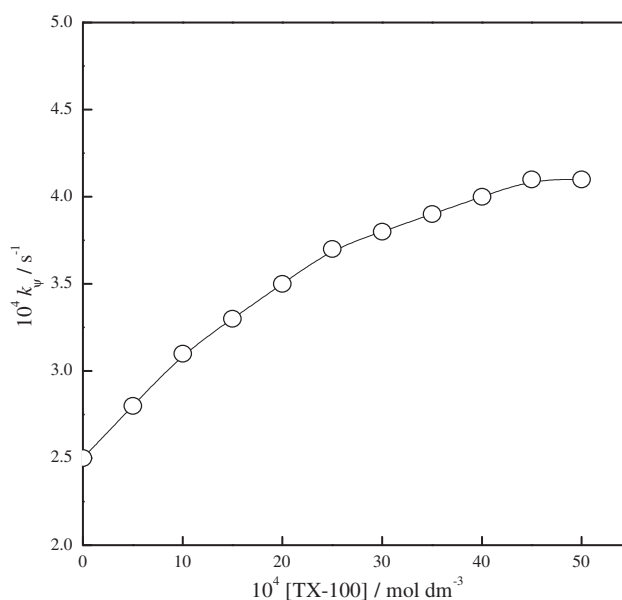

Figure 5 Effect of [TX-100] on the pseudo-first-order rate constant for the reduction of colloidal MnO$_2$ by Gly-Leu. *Reaction conditions*: [MnO$_2$] = 4.0 × 10^{-5} mol dm^{-3}, [Gly-Leu] = 4.0 × 10^{-3} mol dm^{-3}, [HClO$_4$] = 2.0 × 10^{-4} mol dm^{-3}, temperature = 35 °C.

graphically in Figs. 3 and 4. These results indicate that Mn(III) is formed during the reduction. However, attempts to monitor formation of Mn(III) at 470 nm failed to detect any build-up of Mn(III) during the course of the reaction.

5. Reaction in presence of surfactants

To see the role of ionic (SDS and CTAB) and nonionic (TX-100) surfactants on the reaction rate, a series of kinetic runs were carried out with varied concentrations of surfactants at constant [Gly-Leu] (= 4.0 × 10^{-3} mol dm^{-3}), [MnO$_2$] (= 4.0 × 10^{-5} mol dm^{-3}), [HClO$_4$] (= 2.0 × 10^{-4} mol dm^{-3}) and temperature (= 35 °C). Preliminary experiments, which were followed in the presence of anionic surfactant SDS (the

Table 2 Dependence of rate constant on [TX-100] for the reduction of colloidal MnO$_2$ by Gly-Leu.[a]

10^4 [TX-100] (mol dm^{-3})	10^4 k_ψ (s^{-1})
0.0	2.5
5.0	2.8
10.0	3.1
15.0	3.3
20.0	3.5
25.0	3.7
30.0	3.8
35.0	3.9
40.0	4.0
45.0	4.1
50.0	4.1

[a] *Conditions*: [Gly-Leu] = 4.0 × 10^{-3} mol dm^{-3}, [MnO$_2$] = 4.0 × 10^{-5} mol dm^{-3}, [HClO$_4$] = 2.0 × 10^{-4} mol dm^{-3}, temperature = 35 °C.

Table 3 Dependence of rate constant on the factors influencing the reduction of colloidal MnO$_2$ by Gly-Leu in presence of TX-100.[a]

10^3 [Gly-Leu] (mol dm^{-3})	10^5 [MnO$_2$] (mol dm^{-3})	10^4 [HClO$_4$] (mol dm^{-3})	Temperature (°C)	10^4k_{obs} (s^{-1})
1.0	4.0	2.0	35	1.3
2.0				2.5
4.0				2.8
6.0				3.2
8.0				3.4
10.0				3.9
4.0	2.0	2.0	35	6.2
	4.0			2.8
	6.0			2.7
	8.0			2.5
	10.0			2.3
4.0	4.0	1.0	35	2.4
		2.0		2.8
		4.0		3.2
		6.0		3.5
		8.0		3.7
		10.0		4.0
4.0	4.0	2.0	30	2.1
			35	2.8
			40	4.3
			45	5.7
			50	9.2

Activation parameters	
E_a (kJ mol^{-1})	57
$\Delta H^\#$ (kJ mol^{-1})	55
$\Delta S^\#$ (J K^{-1} mol^{-1})	−182
$\Delta G^\#$ (kJ mol^{-1})	112

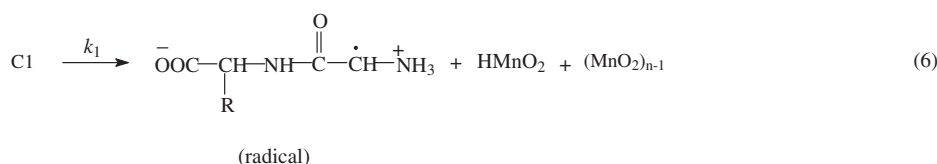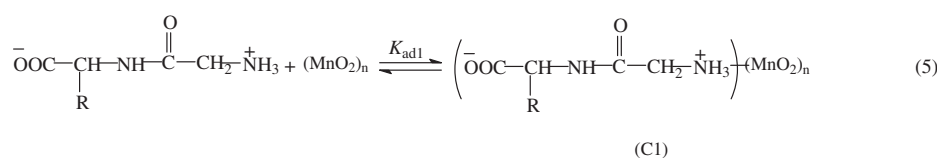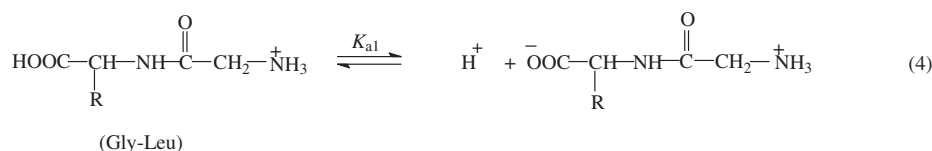[a] *Condition*: [TX-100] = 10.0 × 10^{-4} mol dm^{-3}.

micelles possess net negative charge due to $-OSO_3^-$), indicate that the rate of disappearance of colloidal MnO_2 remained unchanged due to the electrostatic repulsion. On the other hand, precipitate formation was observed in the presence of cationic surfactant CTAB, whereas the nonionic surfactant TX-100 (critical micelle concentration, cmc $= 0.24 \times 10^{-3}$ mol dm^{-3}) showed a catalytic effect on the rate of reaction, (T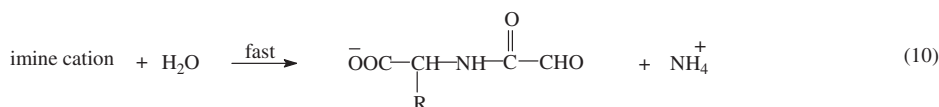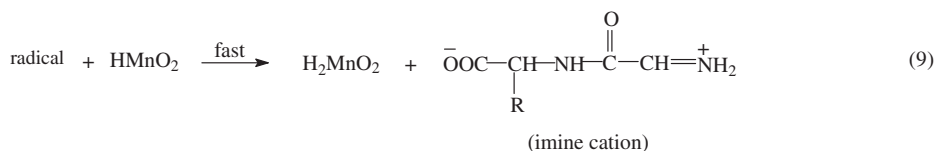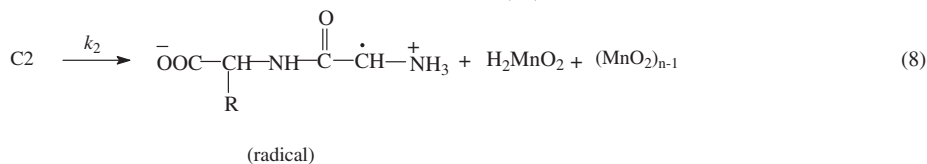able 2) wh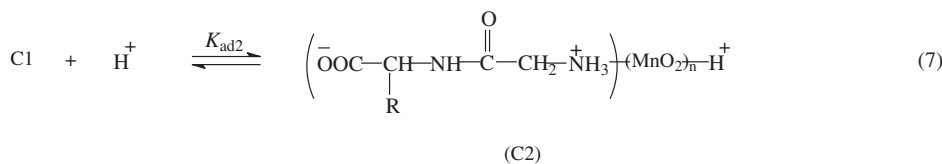ich may be explained in terms of increasing solubilization and association or adsorption of the reactive species (oxidant and reductant) on the surfactant. As the [TX-100] increased, the rate constant increased to a limiting value and then remained constant (Fig. 5).

To confirm whether the mechanism of the reduction of colloidal MnO_2 by Gly-Leu in both aqueous as well as micellar media is similar, different experiments were performed as functions of [Gly-Leu], [MnO_2], and [$HClO_4$] in the presence of

(i) _acid-independent_

$$HOOC\!-\!\overset{\displaystyle}{\underset{\displaystyle R}{CH}}\!-\!NH\!-\!\overset{\displaystyle O}{\overset{\|}{C}}\!-\!CH_2\!-\!\overset{+}{N}H_3 \; \underset{}{\overset{K_{a1}}{\rightleftharpoons}} \; H^+ \;+\; {}^-OOC\!-\!\underset{\displaystyle R}{CH}\!-\!NH\!-\!\overset{\displaystyle O}{\overset{\|}{C}}\!-\!CH_2\!-\!\overset{+}{N}H_3 \qquad (4)$$

(Gly-Leu)

$$^-OOC\!-\!\underset{\displaystyle R}{CH}\!-\!NH\!-\!\overset{\displaystyle O}{\overset{\|}{C}}\!-\!CH_2\!-\!\overset{+}{N}H_3 + (MnO_2)_n \; \overset{K_{ad1}}{\rightleftharpoons} \; \left({}^-OOC\!-\!\underset{\displaystyle R}{CH}\!-\!NH\!-\!\overset{\displaystyle O}{\overset{\|}{C}}\!-\!CH_2\!-\!\overset{+}{N}H_3 \right)\!(MnO_2)_n \qquad (5)$$

(C1)

$$C1 \; \overset{k_1}{\longrightarrow} \; {}^-OOC\!-\!\underset{\displaystyle R}{CH}\!-\!NH\!-\!\overset{\displaystyle O}{\overset{\|}{C}}\!-\!\overset{\displaystyle \bullet}{C}H\!-\!\overset{+}{N}H_3 \;+\; HMnO_2 \;+\; (MnO_2)_{n-1} \qquad (6)$$

(radical)

(ii) _acid-dependent_

$$C1 \;+\; H^+ \; \overset{K_{ad2}}{\rightleftharpoons} \; \left({}^-OOC\!-\!\underset{\displaystyle R}{CH}\!-\!NH\!-\!\overset{\displaystyle O}{\overset{\|}{C}}\!-\!CH_2\!-\!\overset{+}{N}H_3 \right)\!(MnO_2)_n\!-\!H^+ \qquad (7)$$

(C2)

$$C2 \; \overset{k_2}{\longrightarrow} \; {}^-OOC\!-\!\underset{\displaystyle R}{CH}\!-\!NH\!-\!\overset{\displaystyle O}{\overset{\|}{C}}\!-\!\overset{\displaystyle \bullet}{C}H\!-\!\overset{+}{N}H_3 \;+\; H_2MnO_2 \;+\; (MnO_2)_{n-1} \qquad (8)$$

(radical)

$$radical \;+\; HMnO_2 \; \overset{fast}{\longrightarrow} \; H_2MnO_2 \;+\; {}^-OOC\!-\!\underset{\displaystyle R}{CH}\!-\!NH\!-\!\overset{\displaystyle O}{\overset{\|}{C}}\!-\!CH\!\!=\!\!\overset{+}{N}H_2 \qquad (9)$$

(imine cation)

$$imine\ cation \;+\; H_2O \; \overset{fast}{\longrightarrow} \; {}^-OOC\!-\!\underset{\displaystyle R}{CH}\!-\!NH\!-\!\overset{\displaystyle O}{\overset{\|}{C}}\!-\!CHO \;+\; \overset{+}{N}H_4 \qquad (10)$$

$$H_2MnO_2 \;+\; 2\,H^+ \; \overset{fast}{\longrightarrow} \; Mn(II) \;+\; 2H_2O \qquad (11)$$

(where R $= -CH_2CH(CH_3)_2$)

Scheme 1

[TX-100] ($= 10.0 \times 10^{-4}$ mol dm^{-3}) at 35 °C. The order of the reaction with respect to [Gly-Leu], [MnO₂], and [HClO₄] remained unchanged in micellar medium, therefore, it can be concluded that the mechanism of the reaction remains unaltered in the presence of TX-100. Micellar catalysis can be due to environmental changes decreasing the free energy difference between the initial and the transition state and also due to an increase in the frequency of molecular collisions as a consequence of close association of the reactants at the micellar interface. So the activation energy might play a role in micellar catalysis. Therefore, the effect of temperature on the reaction rate in micellar medium was studied to determine the activation energy. The activation energy ($E_a = 57$ kJ mol^{-1}) in micellar medium was found lower than the activation energy ($E_a = 60$ kJ mol^{-1}) in aqueous medium, indicating the reaction to be faster in the presence of surfactant. The other activation parameters ($\Delta H^{\#}$, $\Delta S^{\#}$ and $\Delta G^{\#}$), evaluated by using Eyring equation, are given in Table 3.

6. Mechanism

The oxidation products of Gly-Leu, namely, aldehyde and ammonia, suggest that the reaction center is the terminal amino group. The terminal carboxyl group is far away from the reaction center. Therefore, we can assume that the nature of the terminal carboxyl group, that is, charged or uncharged form, will have the least effect on the reaction rate. This means that the zwitterionic and the cationic forms of Gly-Leu will have the same rate. Only for simplicity, we have used only zwitterionic form of Gly-Leu in the mechanism. On the basis of above results and discussion, the mechanism of the reduction of colloidal MnO₂ by Gly-Leu is given in Scheme 1.

In Scheme 1, Eqs. (5) and (7) represent the adsorption of the active species of Gly-Leu and hydrogen ion on the surface of the colloidal MnO₂ and complex (C1), respectively. Eqs. (6) and (8) are the respective rate determining steps. After adsorption, complexes C1 and C2 decompose to Mn(III)/(II) and radical. Consequently, the radical reacts with Mn(III) and forms imine cation, which is further hydrolyzed to final products (aldehyde and ammonia).

On the basis of the observed rate law (Eq. (2)) and the proposed mechanism (Scheme 1), the following rate equation is derived:

$$v = -\frac{d[\text{MnO}_2]}{dt}$$
$$= \frac{(k_1 K_{ad1} + k_2 K_{ad1} K_{ad2} [\text{H}^+]) [\text{Gly-Leu}] [\text{MnO}_2]}{1 + (K_{ad1} + K_{ad1} K_{ad2} [\text{H}^+]) [\text{Gly-Leu}]} \quad (12)$$

$$k_{obs} = \frac{(k_1 K_{ad1} + k_2 K_{ad1} K_{ad2} [\text{H}^+])[\text{Gly-Leu}]}{1 + (K_{ad1} + k_{ad1} k_{ad2} [\text{H}^+])[\text{Gly-Leu}]} \quad (13)$$

The total reaction rate, derived by the sum of the contributions corresponding to pathways (i) acid-independence and (ii) acid-dependence is:

$$v = \{k'_I + k''_{II}[(\text{H}^+)_s]\} [\text{MnO}_2] [(\text{Gly-Leu})_s] \quad (14)$$

k'_I and k''_{II} are the rate constants corresponding to (i) and (ii) pathways, whereas $(\text{H}^+)_s$ and $(\text{Gly-Leu})_s$ refer to adsorbed species on the colloid surface.

According to Freundlich isotherm the concentration of a species adsorbed on the colloid surface is directly proportional to the concentration of that species in the bulk solution raised to a certain exponent (Parfitti and Rochester, 1983). Adsorption of organic acids onto the surface of colloidal MnO₂ in quasi-equilibrium reactions prior to the redox rate determining steps is widely accepted (Perez-Benito et al., 1996; Khan et al., 2004). Therefore, adsorption isotherm explains the adsorption of Gly-Leu and H⁺ on the surface of the colloidal MnO₂ and C1, respectively.

Applying the Freundlich adsorption isotherm for the present case, we get:

$$[(\text{H}^+)_s] = a[\text{H}^+]^b, \quad (15)$$

and

$$[(\text{Gly-Leu})_s] = a'[\text{Gly-Leu}]^{b'} \quad (16)$$

where a and b are the adsorption parameters for the respective species. Eq. (14) can now be written as:

$$v = \{k'_I a' + k''_{II} aa'[\text{H}^+]^b\} [\text{MnO}_2] [\text{Gly-Leu}]^{b'} \quad (17)$$

The Eq. (17) agrees very well with the experimental results (see Eq. (2)) with $k_I = k'_I a'$ and $k_{II} = k''_{II} aa'$. However, the values of Freundlich adsorption parameters obtained are $b = 0.19$ and $b' = 0.47$, which satisfy the condition of the Freundlich isotherm that the exponents must be a number in the 0–1 interval (Parfitti and Rochester, 1983).

Tuncay et al. (1999) proposed a mathematical model to explain the micellar catalytic effect on the redox reaction by colloidal particles. The same model is used to explain the catalytic effect of TX-100 on the rate of reduction of colloidal MnO₂ by Gly-Leu, according to which:

$$\log k_{\psi} = x \log[\text{TX-100}] - y \quad (18)$$

k_{ψ} is pseudo-first-order rate constant of the reduction of colloidal MnO₂ by Gly-Leu in the presence of TX-100, x and y being
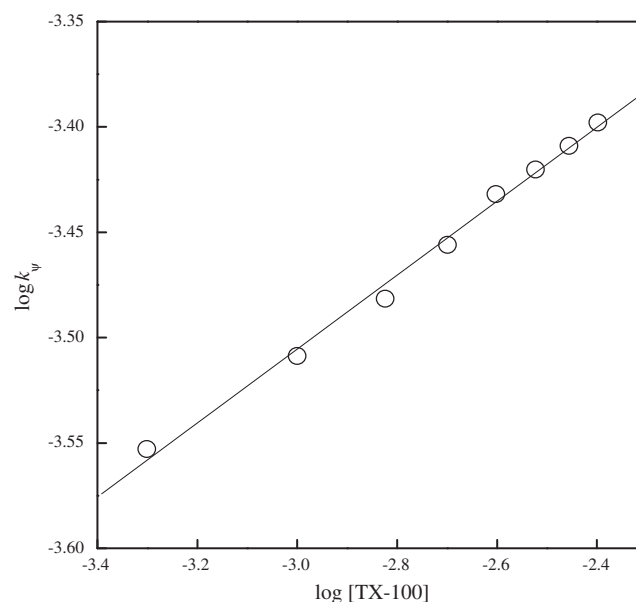
Figure 6 Plot of log k_{ψ} vs. log [TX-100] for the reduction of colloidal MnO₂ by Gly-Leu. *Reaction conditions*: [Gly-Leu] $= 4.0 \times 10^{-3}$ mol dm^{-3}, [HClO₄] $= 2.0 \times 10^{-4}$ mol dm^{-3}, [MnO₂] $= 4.0 \times 10^{-5}$ mol dm^{-3}, temperature = 35 °C.

empirical constants. According to Eq. (18), plot of log k_ψ vs. log [TX-100] should be linear, which was found so (Fig. 6) with slope $x = 0.176$ and intercept $y = 2.979$ ($r = 0.994$).

The following equation, which is similar to Michaelis-Menten type, can be used to explain the catalytic part of the observed results:

$$k_\psi = k_{obs} + \frac{[TX\text{-}100]}{a\,[TX\text{-}100] + b}$$

or

$$k_\psi - k_{obs} = \frac{[TX\text{-}100]}{a\,[TX\text{-}100] + b} \qquad (19)$$

Eq. (19) can be arranged as Lineweaver–Burk form:

$$\frac{1}{(k_\psi - k_{obs})} = a + \frac{b}{[TX\text{-}100]} \qquad (20)$$

The fulfillment of the above relation can be seen in Fig. 7. The values of a and b were calculated from the slope and intercept of Fig. 7 ($a = 0.644 \times 10^3$ s, $b = 2.979$ mol dm^{-3} s) ($r = 0.901$).

7. Role of TX-100

It is, moreover, very clearly apparent from many studies that the hydration of adsorbed molecules plays an important role in the stabilization of dispersions by adsorbed nonionic surfactants (Botsaris et al., 1986). TX-100 is a commercial, polydisperse preparation containing an average of 9.5 oxyethylene units per molecule, which has been widely used as a dispersing agent for colloidal suspensions. Most previous studies have dealt with the adsorption of TX-100 at the solid/aqueous interface but have focused on hydrophilic substrate such as silica (Levitz et al., 1984; Levitz and Van Damme, 1986; Gao

et al., 1984). The TX-100 molecule contains an aromatic nucleus and a highly methylated hydrocarbon chain in the hydrophobic part. On the other hand, colloidal manganese dioxide has no hydrophobic character; therefore, the driving force for adsorption of TX-100 is the H-bond formation between the polar ethylene oxide and the surface of MnO$_2$ sols. It seems reasonable to assume that no significant change occurs in the surface charge density of an MnO$_2$ particle by the adsorption of nonionic surfactant (Mathai and Ottewill, 1962). The NH$_3^+$ groups present in the Gly-Leu molecule, assuming to bind to negatively charged colloidal MnO$_2$, is probably the active point for the Gly-Leu molecules to be adsorbed on the colloidal surface. Normally, there might be competition for adsorption sites between the TX-100 and Gly-Leu molecules. The presence of TX-100 molecules on the interfacial region may be an additional attractive interaction for the Gly-Leu molecules. An important effect of TX-100 molecules on the surface of colloidal MnO$_2$ may be to increase the formation of hydrogen-bonded complexes with Gly-Leu molecules. Due to the presence of a number of donor groups in one TX-100 molecule, multiple H-bonding may take place and the number of bound reactant molecules increase. The surfactant thus, helps in bringing the reactants together into a small volume, which may orient in a manner suitable for the redox reaction followed by rearrangement of TX-100 molecules. A complete explanation of the mechanism as to how TX-100 increased the rate of the reaction is difficult. A great deal remains to be studied about the effect of micelles on the reaction rates having a colloidal particle as one of the reactants.

Figure 7 Plot of $1/(k_\psi - k_{obs})$ vs. $1/[TX\text{-}100]$ for the reduction of colloidal MnO$_2$ by Gly-Leu. *Reaction conditions*: [Gly-Leu] $= 4.0 \times 10^{-3}$ mol dm^{-3}, [HClO$_4$] $= 2.0 \times 10^{-4}$ mol dm^{-3}, [MnO$_2$] $= 4.0 \times 10^{-5}$ mol dm^{-3}, temperature $= 35\,°C$.

References

Akram, M., Altaf, M., Kabir-ud-Din, 2007. Indian J. Chem. 46A, 1427–1431.

Altaf, M., Akram, M., Kabir-ud-Din, 2009. Colloids Surf., B 73, 308–314.

Andrabi, S.M.Z., Khan, Z., 2007. Colloid Polym. Sci. 285, 389–396.

Atwood, J.D., 1990. Inorganic and Organometallic Reaction Mechanisms. Brook/Cole Publishing Company, Monterey, CA.

Barnett, N.W., Hindson, B.J., Lewis, S.W., Jones, P., Worsfold, P.J., 2001. Analyst 126, 1636–1639.

Blokzijl, W., Engberts, J.B.F.N., 1993. Angew. Chem. 105, 1610–1648. Angew. Chem., Int. Ed. 32, 1545–1579.

Botsaris, G.D., Glazman, Yu.M., Bereonja, G.P., 1986. Surf. Solution 6 (III), 1705–1711.

Brown, A.J., Lenehan, C.E., Francis, P.S., Dunstan, D.E., Barnett, N.W., 2007. Talanta 71, 1951–1957.

Davies, G., 1972. Inorg. Chem. 11, 2488–2494.

Davies, K.J.A., 1987. J. Biol. Chem. 262, 9895–9901.

Davies, M.J., 2005. Biochem. Biophys. Acta 1703, 93–109.

Davies, K.J.A., Delsignore, M.E., Lin, S.W., 1987. J. Biol. Chem. 262, 9902–9907.

Deans, R.T., Fu, S., Stocker, R., Davies, M.J., 1997. Biochem. J. 324, 1–18.

Gao, Y., Yue, C., Lu, S., Gu, G., Gu, T., 1984. J. Colloid Interf. Sci. 100, 581–585.

Girgis, M.M., El-Shatoury, S.A., Khalil, Z.H., 1985. Can. J. Chem. 63, 3317–3321.

Giulivi, C., Davies, K.J.A., 1993. J. Biol. Chem. 268, 8752–8759.

Giulivi, C., Davies, K.J.A., 2001. J. Biol. Chem. 276, 24129–24136.

Herszage, J., Afonso, M.D.S., Luther III, G., 2003. Environ. Sci. Technol. 37, 3332–3338.

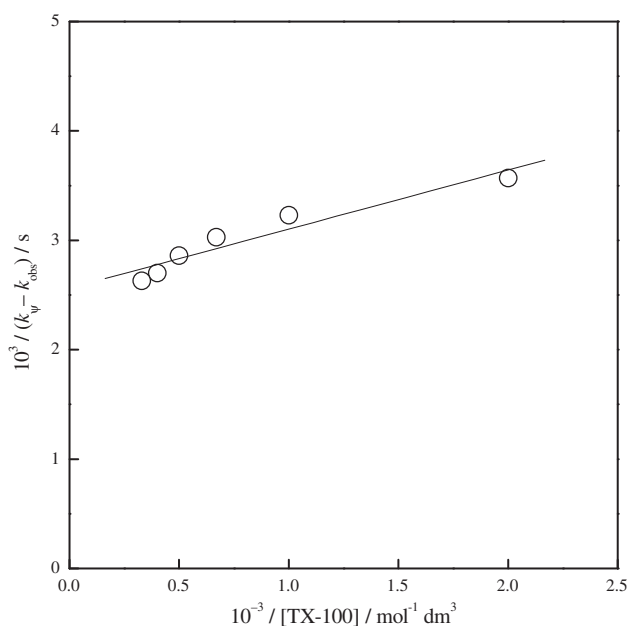Ilyas, M., Malik, M.A., Khan, Z., 2007. Colloid Polym. Sci. 285, 1169–1177.

Jáky, M., Zrinyi, M., 1993. Polyhedron 12, 1271–1275.

Jáky, M., Simándi, L.I., Shafirovich, V.Y., 1984. Inorg. Chim. Acta 90, L39–L41.

Kabir-ud-Din, Fatma, W., Khan, Z., 2004. Colloids Surf., A 234, 159–164.

Kabir-ud-Din, Iqubal, S.M.S., Khan, Z., 2005a. Inorg. React. Mech. 5, 151–166.

Kabir-ud-Din, Iqubal, S.M.S., Khan, Z., 2005b. Colloid Polym. Sci. 284, 276–283.

Kabir-ud-Din, Altaf, M., Akram, M., 2008. J. Disp. Sci. Technol. 29, 809–816.

Khan, Z., Raju Akram, M., Kabir-ud-Din, 2004a. Int. J. Chem. Kinet. 36, 359–366.

Khan, Z., Kumar, P., Kabir-ud-Din, 2004b. Colloids Surf., A 248, 25–31.

Levitz, P., Van Damme, H., 1986. J. Phys. Chem. 90, 1302–1310.

Levitz, P., Van Damme, H., Keravis, D., 1984a. J. Phys. Chem. 88, 2228–2235.

Levitz, P., El Miri, A., Keravis, D., Van Damme, H., 1984b. J. Colloid Interf. Sci. 99, 484–492.

Littler, J.S., 1962. J. Chem. Soc., 832–837.

Mathai, K.G., Ottewill, R.H., 1962. Kolloid Z. Z. Polym. 185, 55–62.

Parfitti, G.D., Rochester, C.H., 1983. In: Parfitti, G.D., Rochester, C.H. (Eds.), Adsorption from Solution at the Solid/Liquid Interface. Academic, New York.

Pastor, T.J., Pastor, F.T., 2000. Talanta 52, 959–970.

Perez-Benito, J.F., Arias, C., 1992. J. Colloid Interf. Sci. 152, 70–84.

Perez-Benito, J.F., Brillas, E., Pouplana, R., 1989. Inorg. Chem. 28, 390–392.

Perez-Benito, J.F., Arias, C., Amat, E., 1996. J. Colloid Interf. Sci. 177, 288–297.

Richens, D.T., Smith, C.G., Sawyer, D.T., 1979. Inorg. Chem. 18, 706–712.

Stadtman, E.R., 1993. Annu. Rev. Biochem. 62, 797–821.

Tuncay, M., Yuce, N., Arlkan, B., Gokturk, S., 1999. Colloids Surf., A 149, 279–284.

Wang, X., Li, Y.D., 2002a. Chem. Commun. 7, 764–765.

Wang, X., Li, Y.D., 2002b. J. Am. Chem. Soc. 124, 2880–2881.

Wang, X., Li, Y.D., 2003. Chem. Eur. J. 9, 300–306.

Wang, G.L., Tang, B., Zhuo, L.H., Ge, J.C., Xue, M., 2006. Eur. J. Inorg. Chem., 2313–2317.

Xiong, Y., Xie, Y., Li, Z., Wu, C., 2003. Chem. Eur. J. 9, 1645–1651.